

Light Bipolarons Stabilized by Peierls Electron-Phonon Coupling

John Sous,^{1,2,3,4,5,*} Monodeep Chakraborty,⁶ Roman V. Krems,² and Mona Berciu^{1,3,†}

¹*Department of Physics and Astronomy, University of British Columbia, Vancouver, British Columbia, Canada, V6T 1Z1*

²*Department of Chemistry, University of British Columbia, Vancouver, British Columbia, Canada, V6T 1Z1*

³*Stewart Blusson Quantum Matter Institute, University of British Columbia, Vancouver, British Columbia, Canada, V6T 1Z4*

⁴*ITAMP, Harvard-Smithsonian Center for Astrophysics, Cambridge, Massachusetts, 02138, USA*

⁵*Department of Physics, Harvard University, Cambridge, Massachusetts, 02138, USA*

⁶*Centre for Theoretical Studies, Indian Institute of Technology, Kharagpur, India*

It is widely accepted that phonon-mediated high-temperature superconductivity is impossible at ambient pressure, because of the very large effective masses of polarons/bipolarons at strong electron-phonon coupling. Here we challenge this belief by showing that strongly bound yet very light bipolarons appear for strong Peierls/Su-Schrieffer-Heeger coupling. These bipolarons also exhibit many other unconventional properties, *e.g.* at strong coupling there are two low-energy bipolaron bands that are stable against strong Coulomb repulsion. Using numerical simulations and analytical arguments, we show that these properties result from the specific form of the phonon-mediated interaction, which is of “pair-hopping” instead of regular density-density type. This unusual effective interaction is bound to have non-trivial consequences for the superconducting state expected to arise at finite carrier concentrations, and should favor a large critical temperature.

Introduction.—Since the discovery of superconductivity in Hg with critical temperature $T_c = 4.2$ K [1], the quest for materials with high T_c has been a central driver of research in condensed matter physics, leading to the discovery of many other superconductors including the unconventional “high”- T_c cuprate [2] and iron-based [3, 4] families, besides many conventional and unconventional low- T_c ones.

Conventional low- T_c superconductivity is understood to be a consequence of electron-phonon coupling [5, 6]: Exchange of phonons binds electrons into Cooper pairs [7] which condense into a superfluid. While there is no proven theory of high- T_c superconductivity, it is widely accepted that phonon-mediated superconductivity cannot exhibit high T_c (at ambient pressure). High T_c would require strong electron-phonon coupling, but in this limit the electrons become dressed by clouds of phonons forming polarons, with a renormalized effective mass [8–22]. As the coupling strength increases, the effective mass grows faster than the phonon-mediated binding, resulting in suppression of T_c [23]. In other words, it is generally believed impossible to form bipolarons (polaron pairs bound by phonon exchange) that remain light at strong electron-phonon coupling, making high- T_c bipolaronic superconductivity very unlikely [23], [24].

Such arguments, however, are based on studies of the Holstein [13] and Fröhlich [10, 12] models. There, phonons modulate the potential energy of the electrons, which explains why polarons and bipolarons become heavier as the coupling strength increases. On the other hand, the coupling to phonons may also modulate the hopping integrals, as described by the Peierls model [25–27] (known as the Su-Schrieffer-Heeger (SSH) model for

polyacetylene [28, 29]). Recently, it was shown that single polarons in this latter class of models can be light at strong coupling strengths [30].

Here we study for the first time phonon-mediated binding of electrons into bipolarons in the Peierls model. We show that Peierls electron-phonon coupling leads to strong phonon-mediated attraction between electrons, which results in the formation of strongly bound yet very light bipolarons: Their mass at strong coupling is close to twice the free electron mass. Such light bipolarons are expected to condense into a superfluid at very high temperatures [23, 39]. Our work thus points to a new direction in the search for high- T_c superconductors: Designing materials with electron-phonon coupling predominantly of the Peierls-type can lead to phonon-mediated superconductivity at high temperatures.

Model and methods.—We study the singlet state of two spin- $\frac{1}{2}$ fermions in an infinite one-dimensional chain described by the Hamiltonian $\mathcal{H} = \mathcal{H}_e + \mathcal{H}_{ph} + \hat{V}_{e-ph}$, where:

$$\mathcal{H}_e = -t \sum_{i,\sigma} \left(c_{i,\sigma}^\dagger c_{i+1,\sigma} + h.c. \right) + \sum_i U(\delta) \hat{n}_{i,\uparrow} \hat{n}_{i+\delta,\downarrow} \quad (1)$$

is the extended Hubbard model of bare electrons with on-site $U(0) = U$ and nearest-neighbor $U(1) = V$ screened repulsion, i is the site index and $\hat{n}_{i,\sigma} = c_{i,\sigma}^\dagger c_{i,\sigma}$ counts particles with spin σ at site i . $\mathcal{H}_{ph} = \Omega \sum_i b_i^\dagger b_i$ (in units of \hbar) is the phonon Hamiltonian describing a single Einstein mode with frequency Ω , and

$$\hat{V}_{e-ph} = g \sum_{i,\sigma} \left(c_{i,\sigma}^\dagger c_{i+1,\sigma} + h.c. \right) \left(b_i^\dagger + b_i - b_{i+1}^\dagger - b_{i+1} \right) \quad (2)$$

is the Peierls/SSH electron-phonon coupling [30]. We characterize the electron-phonon strength using the dimensionless effective coupling $\lambda = 2g^2/(\Omega t)$. We

* jsous@phas.ubc.ca

† berciu@phas.ubc.ca

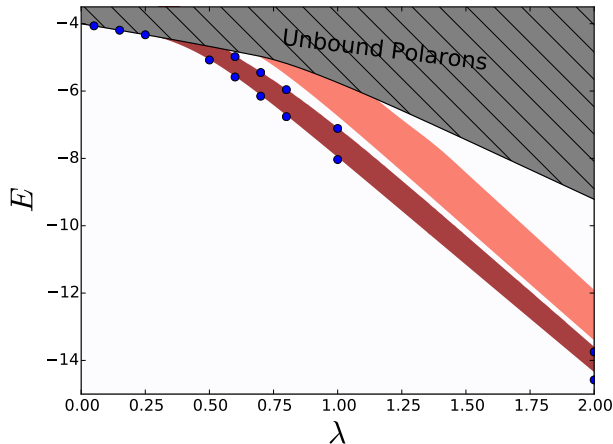


FIG. 1. (Color online) Two-polaron phase diagram for $U(\delta) = 0$ and $\Omega = 3$. The diagram represents the evolution of the low-energy region of the singlet sector with λ . Energies are in units of t . The dimensionless effective coupling is $\lambda = 2g^2/(\Omega t)$. The shaded grey area shows the lower part of the two-polaron continuum. The dark red region represents the lowest energy bipolaron band, while the salmon region represents the higher energy bipolaron band. These results were obtained with MA and are in good agreement with VED results (blue circles) shown for the low-energy bipolaron.

investigate the singlet eigenstates using variational exact diagonalization (VED) [31–33] and an extension of the Momentum Average (MA) approach [22, 30, 34–36].

Numerical results.—We first set $U(\delta) = 0$ and investigate the stability and properties of the resulting bipolarons. The role played by $U(\delta)$ is discussed later.

Figure 1 shows the evolution with λ of the low-energy region of the singlet sector, for $U(\delta) = 0$ and $\Omega = 3$ (all energies are in units of $t = 1$). The shaded grey area shows the lower part of the two-polaron continuum: these states describe two unbound polarons, their energies being the convolution of two single polaron spectra. The dark red region shows the location of the lowest bipolaron band. VED confirms its existence for all $\lambda > 0$, although for weak coupling $\lambda \lesssim 0.3$, the bipolaron ground state lies just below the continuum and cannot be resolved on this scale. With increasing λ , the bipolaron band moves further below the continuum and for $\lambda \gtrsim 0.57$ it becomes fully separated from it. For strong coupling $\lambda > 1$, this band is accompanied by a higher energy bipolaron band (salmon-colored region), whose evolution with λ closely mirrors that of the lower band, suggesting a common origin. Note that this second band lies below the bipolaron+one-phonon continuum (not shown) that starts at Ω above the ground state, and therefore it is an infinitely lived bipolaron.

Clearly the bandwidths of both bipolaron bands are wide even at extremely strong couplings $\lambda \sim 2$ (this persists for $\lambda > 2$ but such values are unphysical), showing that the bipolarons remain light even when very

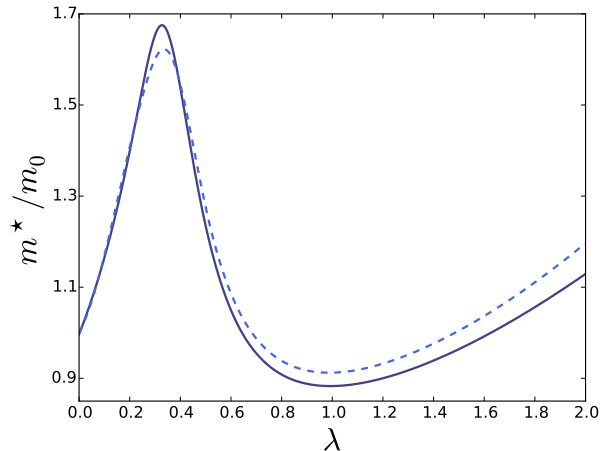


FIG. 2. (Color online) Dependence of the effective mass of the low-energy bipolaron on λ , for $U(\delta) = 0$ and $\Omega = 3.0$. $m_0 = 2m_e$ is twice the free electron mass. The bipolaron's effective mass is defined as $m^* = \left(\frac{\partial^2 E_{BP}(K)}{\partial K^2} \right)^{-1} \Big|_{K=K_{GS}}$. The solid (dashed) lines are VED (MA) results. Note that $m^* \sim 2m_e$ in the strongly coupled regime, $\lambda > 1$.

strongly bound. This is further confirmed in Figure 2, where we plot the low-energy bipolaron's effective mass m^* , in units of two free particle masses, $m_0 = 2m_e = \hbar^2/ta^2$, where a is the lattice constant. m^* varies non-monotonically with λ , with a peak at $\lambda \sim 0.325$ where the bipolaron ground state energy starts to drop fast below the lower edge of the two-polaron continuum (see Figure 1), *i.e.* the bipolaron crosses over into the strongly bound regime. Importantly, the ratio m^*/m_0 stays close to 1 for $\lambda \gtrsim 1$. In other words, the Peierls bipolaron's effective mass remains comparable to that of a pair of free fermions even at very strong coupling $\lambda = 2$. For comparison, for the same Ω and $\lambda = 2$, the Holstein bipolaron's bandwidth is 0.0135, *i.e.* its mass is larger by about two orders of magnitude.

The existence of strongly bound yet light Peierls bipolarons at strong coupling is our central result.

We now discuss the second bipolaron band. For reference, we note that the one-dimensional Holstein and Fröhlich models host only one bipolaron band within Ω of the ground-state energy (if $U = 0$) [32]. This is precisely what is generically expected. For Holstein coupling, the phonon-mediated effective interaction can be modeled as an effective on-site attraction $-\Delta E \sum_i \hat{n}_{i\uparrow} \hat{n}_{i\downarrow}$, where $\Delta E \rightarrow 2g^2/\Omega$ as $\lambda \rightarrow \infty$ [31, 32]. In one dimension, such effective on-site attraction binds two fermions into a singlet state, but there is only one bound state. The existence of a second bipolaron state is thus very surprising, and points to a new mechanism behind pairing.

To understand this new physics, we first consider the dispersion of the lowest energy bipolaron, and its evolution with increasing λ . This is shown in Figure 3

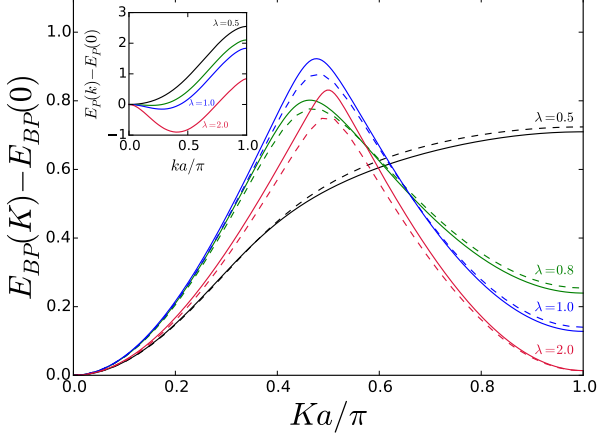


FIG. 3. (Color online) Dispersion $E_{BP}(K) - E_{BP}(0)$ of the low-energy bipolaron, for various values of $\lambda = 2g^2/(\Omega t)$ at $U(\delta) = 0$ and $\Omega = 3$. The inset shows the polaron dispersion $E_P(k) - E_P(0)$ for the same parameters. All energies are in units of t . In the main figure, solid lines are VED results and dashed lines are MA results. Results in the inset were obtained with MA, and are in good agreement with numerical results [30].

for the positive half of the Brillouin zone. The curves have been shifted for ease of comparison (their absolute positions can be inferred from Figure 1). The inset shows the polaron dispersions for the same coupling parameters.

At couplings $\lambda \leq 0.5$ where only this bipolaron band exists, the dispersion has the standard behavior, being monotonically increasing with K . For larger λ , the dispersion has a rather unusual shape, strongly peaked near $Ka = \frac{\pi}{2}$. This shape is highly suggestive of an avoided crossing with a band located above (the second bipolaron state that emerges at these couplings). This is confirmed when we plot both bands for $\lambda = 2$ in Figure 4. The gap that opens between the two bands varies only weakly with λ , see Figure 1. This behavior suggests the existence of two bound states with different symmetries, coupled by a λ -independent symmetry-breaking term.

Analytical arguments.—To unravel the pairing mechanism and explain the origin of the two bipolaron states and their avoided crossing, we consider the anti-adiabatic limit $\Omega \gg t, g$. We obtain analytical results by projecting out the high-energy Hilbert subspaces with one or more phonons [37]. Note that strong-coupling $\lambda \gg 1$ is included within the anti-adiabatic regime if $t \ll g \ll \Omega$ such that $g^2 \gg \Omega t$.

As discussed in Ref. [30], the effective Hamiltonian in the single particle sector is

$$\hat{h}_1 = -\epsilon_0 \sum_{i,\sigma} \hat{n}_{i,\sigma} - \sum_{i,\sigma} \left(t c_{i,\sigma}^\dagger c_{i+1,\sigma} - t_2 c_{i,\sigma}^\dagger c_{i+2,\sigma} + h.c. \right)$$

In addition to the nearest-neighbor bare particle hopping, \hat{h}_1 contains the polaron formation energy $\epsilon_0 = 4g^2/\Omega$,

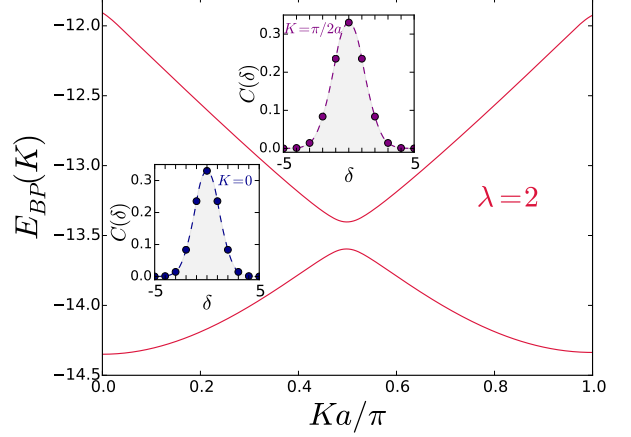


FIG. 4. (Color online) Dispersion $E_{BP}(K)$ of both bipolaron bands, for $U(\delta) = 0$, $\Omega = 3$ and $\lambda = 2$, showing an avoided crossing. $E_{BP}(K)$ is in units of t . These are MA results. The insets show the low-energy bipolaron spatial correlation function $C(\delta) = \langle \Psi_{BP} | \frac{1}{N} \sum_i \hat{n}_{i,\uparrow} \hat{n}_{i+\delta,\downarrow} | \Psi_{BP} \rangle$ at $\lambda = 2$ for $K = 0$ and $K = \pi/2a$ obtained with VED. In both cases, the electrons in the bipolaron wavefunction are found with large probability to be up to two sites apart.

and a dynamically generated next-nearest-neighbor hopping $t_2 = g^2/\Omega$ resulting from virtual emission and subsequent absorption of a phonon by the particle, as it hops on and off an intermediate site. This term becomes dominant for large λ and explains the change in the shape of the polaron dispersion $E_P(k) = -\epsilon_0 - 2t \cos(ka) + 2t_2 \cos(2ka)$ observed in the inset of Figure 3 (for detailed discussions see Ref. [30]).

In the singlet sector, we find that the effective two-particle Hamiltonian is: $\hat{h}_{2,s} = \hat{h}_1 + \hat{U}_{0,2} + \hat{U}_1$. The additional terms describe short-range phonon-mediated interactions between the polarons. Specifically

$$\begin{aligned} \hat{U}_{0,2} = & -T_{0,0} \sum_i \left[c_{i-1,\uparrow}^\dagger c_{i-1,\downarrow}^\dagger c_{i,\downarrow} c_{i,\uparrow} + h.c. \right] \\ & + T_{0,2} \sum_i \left[\left(c_{i+1,\uparrow}^\dagger c_{i-1,\downarrow}^\dagger - c_{i+1,\downarrow}^\dagger c_{i-1,\uparrow}^\dagger \right) c_{i,\downarrow} c_{i,\uparrow} + h.c. \right] \end{aligned}$$

describes nearest-neighbor “pair-hopping” of an on-site singlet with $T_{0,0} = \frac{4g^2}{\Omega}$, and transitions between on-site and next-nearest-neighbor singlets with $T_{0,2} = \frac{2g^2}{\Omega}$. They arise through emission and absorption of a phonon, e.g. $c_{i,\uparrow}^\dagger c_{i,\downarrow}^\dagger |0\rangle \xrightarrow{\hat{V}_{e-\text{ph}}} c_{i+1,\uparrow}^\dagger c_{i,\downarrow}^\dagger b_{i+1}^\dagger |0\rangle \xrightarrow{\hat{V}_{e-\text{ph}}} c_{i+1,\uparrow}^\dagger c_{i+1,\downarrow}^\dagger |0\rangle$ allows one particle to hop by emitting a phonon, then the second particle absorbs the phonon and hops to its partner’s new site. This is one of the processes contributing to $T_{0,0}$; all relevant processes can be similarly inferred.

The other effective interaction term

$$\hat{U}_1 = +T_{1,1} \sum_{i,\sigma} \left[c_{i+1,\sigma}^\dagger c_{i+2,-\sigma}^\dagger c_{i+1,-\sigma} c_{i,\sigma} + h.c. \right] \\ + J \sum_{i,\sigma} c_{i+1,\sigma}^\dagger c_{i,-\sigma}^\dagger c_{i,\sigma} c_{i+1,-\sigma}$$

acts when the particles are on adjacent sites and describes the pair-hopping of a nearest-neighbor singlet with $T_{1,1} = \frac{2g^2}{\Omega}$, and an antiferromagnetic xy exchange with $J = \frac{4g^2}{\Omega}$.

Note that none of these terms are of the density-density type of interaction that is assumed to be the functional form for phonon-mediated effective interactions. More specifically, these terms can be written in the form $\sum_{k,k',q} u(k+k',q) c_{k+q,\uparrow}^\dagger c_{k'-q,\downarrow}^\dagger c_{k',\downarrow} c_{k,\uparrow}$ allowed by translational invariance. The interaction vertex, $u(k+k',q)$, depends not only on the exchanged momentum, q , as is usually assumed to be the case, but also on the total momentum of the interacting pair, $k+k'$. It is therefore important to understand the consequences of such interactions, for example, how they affect the properties of BCS- or Bose-Einstein-Condensate(BEC)-type superconductors. We leave such studies for future work.

The origin of the two different symmetry states leading to the two bipolaron bands is now clear. First, let us set $t = 0$. In this case, the low-energy Hilbert subspace factorizes into two sectors, with the particles being separated either by an even or by an odd number of sites; the remaining terms in the Hamiltonian do not mix these subspaces. To solve for bound states, we calculate the two-particle propagator [38] and check for discrete poles appearing below the continuum. We find that $\hat{U}_{0,2}$ and \hat{U}_1 can lead to the appearance of a bound state in their respective subspace. The former has a monotonically increasing dispersion, $E_{\text{even}}(K) = -2\epsilon_0 - 2T_{0,0} \cos(Ka) + \mu(K)$, where $\mu(K) = \frac{F_{\text{even}}(K)}{2\theta(K)} - \frac{1}{2} \sqrt{(\frac{F_{\text{even}}(K)}{\theta(K)})^2 + 4\zeta(K)}$, with $F_{\text{even}}(K) = 2T_{0,0} \cos(Ka)$, $\theta(K) = 1 - \frac{(f_2(K))^2}{\alpha(K)}$, $\zeta(K) = \frac{\alpha(K)}{\theta(K)}$; $f_2(K) = 2t_2 \cos(Ka)$ and $\alpha(K) = 2(T_{0,2} + f_2(K))^2$. The latter has a monotonically decreasing dispersion, $E_{\text{odd}}(K) = -2\epsilon_0 - J + 2(t_2 + T_{1,1}) \cos(Ka) + \kappa(K)$, with $\kappa(K) = \frac{(f_2(K))^2}{f_2(K) + F_{\text{odd}}(K)}$, where $F_{\text{odd}}(K) = -J + 2T_{1,1} \cos(Ka)$. Note that both these energies are controlled by the energy scale g^2/Ω , explaining why they evolve similarly with increasing λ . When t is turned on, the nearest-neighbor hopping term breaks this symmetry and leads to the avoided crossing, and hence the two bipolaron bands with unusual dispersions shown in Figure 4.

We now address the role of the Coulomb repulsion $U(\delta)$. In Figure 5, we display the critical value U_c above which bipolarons dissociate into unbound polarons, for the Peierls/SSH (solid lines) and Holstein (dashed line) models. Clearly, U_c is much larger for Peierls bipolarons than for Holstein bipolarons, even with a strong nearest-

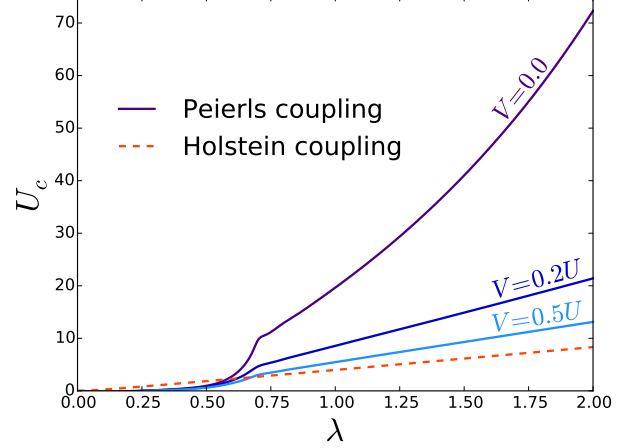


FIG. 5. (Color online) U_c - λ stability diagram for the Peierls/SSH (solid lines) and Holstein (dashed line) bipolarons at $\Omega = 3$. U_c is in units of t . For the Peierls/SSH coupling, $\lambda = 2g^2/(\Omega t)$, while for the Holstein coupling, $\lambda = g_H^2/(2\Omega t)$, where g_H is the Holstein electron-phonon coupling. These are VED results, and reveal a qualitative difference between the stability of the two types of bipolarons at strong coupling $\lambda > 1$. The Peierls bipolaron remains more stable than the Holstein bipolaron even in the presence of a screened nearest-neighbor Coulomb repulsion $V = 0.2U$ and $V = 0.5U$.

neighbor $V = 0.5U$. This is yet another qualitative difference between the two models.

In the Holstein model, U directly competes with the on-site attraction ΔE mediated by phonons. A smooth crossover from an on-site bipolaron to a weakly bound bipolaron with the particles on neighboring sites is observed for $U \sim \Delta E$, and a somewhat larger U suffices to dissociate the bipolaron [31].

For the Peierls/SSH coupling, consider again the anti-adiabatic limit with $t = 0$. Here, for $V = 0$, a sufficiently large U will destabilize the bound state in the even sector, but will have much less effect on the bound state of the odd sector. Hybridization due to a finite t will then result in a low-energy bipolaron similar to the bound state of the odd sector. Consequently, one expects a stable bipolaron even for large values of U . Moreover, for a sufficiently large U value, one expects a transition to a bipolaron with ground state momentum $K_{GS} = \pi/a$, favored by the odd bound state. Indeed, we verified this behavior in the anti-adiabatic limit (not shown). Including a nearest-neighbor repulsion $V \sim U$ further suppresses U_c , as verified in Figure 5.

Away from the anti-adiabatic limit, see Figure 5, we find that the t -controlled mixing between even and odd bound states suffices to destabilize both states, at large enough $U > U_c$. Still, U_c is larger than for the Holstein model even for a very strong $V/U = 0.5$.

The Peierls bipolarons are thus stable in a much wider range of repulsive U than the Holstein bipolarons. This

is a direct consequence of the existence of the two bound states with different symmetries, one of which is only weakly affected by large U (at $t = 0$).

Summary and discussion.—We have demonstrated the existence of strongly bound yet light Peierls bipolarons, stable against large values of the screened Coulomb repulsion. The light bipolaron is a consequence of the Peierls-type coupling, not of special circumstances like in Ref. [39], making our conclusions applicable to a large class of systems. We explained that pairing is mediated by pair-hopping terms instead of the customary attractive Hubbard-like terms. This unusual attraction binds two low-energy bipolaron states, instead of one. As a result of an avoided crossing, these Peierls bipolarons have unique dispersions.

The binding mechanism poses questions about the nature of superconductivity at finite carrier densities in higher dimensions: Light bipolarons should condense into a BEC-type superconductor with high T_c . This should be relevant to conjugated polymers [28, 29, 40], organic semiconductors [41–44], some oxides [45, 46], and engineered quantum simulators [47–52]. Recent work claims a record T_c for superconductivity in doped organic p-terphenyl molecules [53, 54], where the Peierls coupling is important, and attributes it to a possible bipolaronic mechanism [53]. Similarly, our work may be relevant to understanding electron-phonon driven superconductivity in SrTiO_3 [55], especially given its recently uncovered

one-dimensional nature [56], in magic-angle graphene [57], and layered MoS_2 [58].

To validate our proposed new pathway to high-temperature superconductivity, a detailed understanding of Peierls/SSH couplings and their interplay with Coulomb repulsion at finite carrier concentrations is required, see [59, 60] for recent studies.

All these considerations indicate that the issue of phonon-mediated high-temperature superconductivity must be revisited.

ACKNOWLEDGMENTS

We thank Daniel Dessau and Mirko Möller for useful discussions. This work was supported by the Natural Sciences and Engineering Research Council of Canada (NSERC) (J.S., R.V.K. and M.B.) and the Stewart Blusson Quantum Matter Institute (SBQMI) (J.S. and M.B.). J.S. is also supported by a visiting student fellowship at the Institute for Theoretical Atomic, Molecular, and Optical Physics (ITAMP) at Harvard University and the Smithsonian Astrophysical Observatory. M.C. appreciates access to the computing facilities of the DST-FIST (phase-II) project installed in the Department of Physics, Indian Institute of Technology (IIT), Kharagpur, India.

-
- [1] H. Kamerlingh-Onnes, Comm. Phys. Lab. Univ. Leiden 124 (1911).
 - [2] J. G. Bednorz and K. A. Müller, Z. Phys. B **64**, 189 (1986).
 - [3] Y. Kamihara, T. Watanabe, M. Hirano, and H. Hosono, J. Am. Chem. Soc. **130**, 3296 (2008).
 - [4] H. Takahashi, K. Igawa, K. Arii, Y. Kamihara, M. Hirano, and H. Hosono, Nature **453**, 376 EP (2008).
 - [5] J. Bardeen, L. N. Cooper, and J. R. Schrieffer, Phys. Rev. **106**, 162 (1957).
 - [6] J. Bardeen, L. N. Cooper, and J. R. Schrieffer, Phys. Rev. **108**, 1175 (1957).
 - [7] L. N. Cooper, Phys. Rev. **104**, 1189 (1956).
 - [8] L. Landau, Phys. Z. Sowjetunion **3**, 644 (1933).
 - [9] L. Landau and S. Pekar, J. Exp. Theor. Phys **18**, 419 (1948).
 - [10] H. Fröhlich, H. Pelzer, and S. Zienau, Philos. Mag. **41**, 221 (1950).
 - [11] S. Tyablikov, Zh. Eksp. Teor. Fiz **23**, 381 (1952).
 - [12] H. Fröhlich, Adv. Phys. **3**, 325 (1954).
 - [13] T. Holstein, Ann. Phys. **281**, 725 (2000).
 - [14] R. P. Feynman, Phys. Rev. **97**, 660 (1955).
 - [15] R. Feynman, R. Hellwarth, C. Iddings, and P. Platzman, Phys. Rev. **127**, 1004 (1962).
 - [16] N. V. Prokof'ev and B. V. Svistunov, Phys. Rev. Lett. **81**, 2514 (1998).
 - [17] N. V. Prokof'ev and B. V. Svistunov, Phys. Rev. Lett. **81**, 2514 (1998).
 - [18] P. E. Kornilovitch, Phys. Rev. Lett. **81**, 5382 (1998).
 - [19] J. Bonča, S. A. Trugman, and I. Batistić, Phys. Rev. B **60**, 1633 (1999).
 - [20] L.-C. Ku, S. A. Trugman, and J. Bonča, Phys. Rev. B **65**, 174306 (2002).
 - [21] J. P. Hague, P. E. Kornilovitch, A. S. Alexandrov, and J. H. Samson, Phys. Rev. B **73**, 054303 (2006).
 - [22] G. L. Goodvin, M. Berciu, and G. A. Sawatzky, Phys. Rev. B **74**, 245104 (2006).
 - [23] B. K. Chakraverty, J. Ranninger, and D. Feinberg, Phys. Rev. Lett. **81**, 433 (1998).
 - [24] High- T_c bipolaronic superconductivity may be possible in very special circumstances like in Ref. [39].
 - [25] S. Barišić, J. Labbé, and J. Friedel, Phys. Rev. Lett. **25**, 919 (1970).
 - [26] S. Barišić, Phys. Rev. B **5**, 932 (1972).
 - [27] S. Barišić, Phys. Rev. B **5**, 941 (1972).
 - [28] W. P. Su, J. R. Schrieffer, and A. J. Heeger, Phys. Rev. Lett. **42**, 1698 (1979).
 - [29] A. J. Heeger, S. Kivelson, J. R. Schrieffer, and W. P. Su, Rev. Mod. Phys. **60**, 781 (1988).
 - [30] D. J. J. Marchand, G. De Filippis, V. Cataudella, M. Berciu, N. Nagaosa, N. V. Prokof'ev, A. S. Mishchenko, and P. C. E. Stamp, Phys. Rev. Lett. **105**, 266605 (2010).
 - [31] J. Bonča, T. Katrašnik, and S. A. Trugman, Phys. Rev. Lett. **84**, 3153 (2000).
 - [32] J. Bonča and S. A. Trugman, Phys. Rev. B **64**, 094507 (2001).
 - [33] M. Chakraborty, B. I. Min, A. Chakrabarti, and A. N.

- Das, Phys. Rev. B **85**, 245127 (2012).
- [34] M. Berciu, Phys. Rev. Lett. **97**, 036402 (2006).
 - [35] J. Sous, M. Chakraborty, C. P. J. Adolphs, R. V. Krems, and M. Berciu, Sci. Rep. **7**, 1169 (2017).
 - [36] J. Sous *et al.*, in preparation.
 - [37] M. Takahashi, J. Phys. C: Solid State Phys. **10**, 1289 (1977).
 - [38] M. Berciu, Phys. Rev. Lett. **107**, 246403 (2011) .
 - [39] J. P. Hague, P. E. Kornilovitch, J. H. Samson, and A. S. Alexandrov, Phys. Rev. Lett. **98**, 037002 (2007) .
 - [40] A. De Sio, F. Troiani, M. Maiuri, J. Réhault, E. Sommer, J. Lim, S. F. Huelga, M. B. Plenio, C. A. Rozzi, G. Cerullo, E. Molinari, and C. Lienau, Nat. Commun. **7**, 13742 (2016).
 - [41] S. Nelson, Y.-Y. Lin, D. Gundlach, and T. Jackson, Appl. Phys. Lett. **72**, 1854 (1998).
 - [42] A. Troisi and G. Orlandi, Phys. Rev. Lett. **96**, 086601 (2006).
 - [43] G. De Filippis, V. Cataudella, A. S. Mishchenko, N. Nagaosa, A. Fierro, and A. de Candia, Phys. Rev. Lett. **114**, 086601 (2015).
 - [44] S. Fratini, S. Ciuchi, D. Mayou, G. T. de Laissardiere, and A. Troisi, Nat. Mater. **16**, 998 (2017).
 - [45] S. J. Pearton, W. H. Heo, M. Ivill, D. P. Norton, and T. Steiner, Semicond. Sci. Technol. **19**, R59 (2004).
 - [46] S. Johnston, A. Mukherjee, I. Elfimov, M. Berciu, and G. A. Sawatzky, Phys. Rev. Lett. **112**, 106404 (2014).
 - [47] F. Herrera and R. V. Krems, Phys. Rev. A **84**, 051401 (2011).
 - [48] F. Herrera, K. W. Madison, R. V. Krems, and M. Berciu, Phys. Rev. Lett. **110**, 223002 (2013).
 - [49] J. P. Hague and C. MacCormick, New J. Phys. **14**, 033019 (2012).
 - [50] S. Mostame, P. Rebentrost, A. Eisfeld, A. J. Kerman, D. I. Tsomokos, and A. Aspuru-Guzik, New J. Phys. **14**, 105013 (2012).
 - [51] V. M. Stojanović, M. Vanević, E. Demler, and L. Tian, Phys. Rev. B **89**, 144508 (2014).
 - [52] Z. Lan and C. Lobo, Phys. Rev. A **90**, 033627 (2014).
 - [53] R.-S. Wang, Y. Gao, Z.-B. Huang, and X.-J. Chen, arXiv preprint arXiv:1703.06641 (2017).
 - [54] H. Li, X. Zhou, S. Parham, T. Nummy, J. Griffith, K. Gordon, E. L. Chronister, and D. Dessau, arXiv preprint arXiv:1704.04230 (2018).
 - [55] J. F. Schooley, W. R. Hosler, and M. L. Cohen, Phys. Rev. Lett. **12**, 474 (1964).
 - [56] Y.-Y. Pai, H. Lee, J.-W. Lee, A. Annadi, G. Cheng, S. Lu, M. Tomczyk, M. Huang, C.-B. Eom, P. Irvin, and J. Levy, Phys. Rev. Lett. **120**, 147001 (2018).
 - [57] Y. Cao, V. Fatemi, S. Fang, K. Watanabe, T. Taniguchi, E. Kaxiras, and P. Jarillo-Herrero, Nature **556**, 43 EP (2018).
 - [58] M. Kang, S. W. Jung, W. J. Shin, Y. Sohn, S. H. Ryu, T. K. Kim, M. Hoesch, and K. S. Kim, Nat. Mater. (2018).
 - [59] M. Hohenadler, Phys. Rev. Lett. **117**, 206404 (2016).
 - [60] Y. Werman, S. A. Kivelson, and E. Berg, npj Quantum Mater. **2**, 7 (2017).